RSC Advances

PAPER

View Article Online
View Journal | View Issue

Check for updates

Cite this: *RSC Adv.*, 2025, **15**, 13882

Development and application of coffee husk-based polyaniline composite (CF@PANi) for enhanced ammonium removal from aqueous solutions

Thuy-Tien Do,[a] Huu-Tap Van,*[b] The-Duyen Nguyen,[a] Thi-Huyen Nguyen[a] and Xuan-Bach Nguyen[a]

This study focuses on the development and evaluation of a novel composite material, designated as CF@PANi, which integrates coffee husk and polyaniline for the purpose of ammonium adsorption from aqueous solutions. The composite was synthesized under optimized conditions and characterized using various analytical techniques. The results from SEM and EDS indicated significant structural and compositional changes following the adsorption process, including an increase in porosity and a notable rise in nitrogen content from 6.35% to 17.24%, thereby confirming effective ammonium uptake. BET analysis revealed that the synthesized composite possesses a mesoporous structure with a surface area of 7.0642 $m^2\ g^{-1}$. FTIR spectroscopy identified active functional groups, such as amine (–NH, $–NH_2$) and hydroxyl (–OH), critical for adsorption. Batch adsorption experiments were conducted to assess the effects of various parameters, including pH, adsorbent dosage, contact time and initial ammonium concentration, on adsorption performance. The optimal conditions for ammonium adsorption were determined to be at a pH of 7, with a PANi : CF ratio of 1 : 2 and a contact time of 40 min, achieving a maximum adsorption capacity (q_e) of 25.05 mg g^{-1}, as predicted by the Langmuir isotherm model. Kinetic studies indicated that the adsorption process follows a pseudo-second-order model. The mechanistic analysis highlighted key processes involved in ammonium adsorption, including electrostatic attraction, cation exchange, surface complexation, physical adsorption, and cation–π interactions.

Received 9th February 2025
Accepted 25th April 2025

DOI: 10.1039/d5ra00949a

rsc.li/rsc-advances

Open Access Article. Published on 30 April 2025. Downloaded on 6/15/2026 5:50:00 AM.
This article is licensed under a Creative Commons Attribution-NonCommercial 3.0 Unported Licence.

Introduction

Ammonium (NH_4^+) pollution in water bodies and wastewater effluents is a significant environmental concern due to its detrimental impacts on aquatic ecosystems and human health. A substantial body of research indicates that agricultural activities contribute to ammonium pollution in water bodies.[1–3] Studies have shown that crops absorb approximately 50% of applied nitrogen fertilizers, with the remaining portion susceptible to runoff and transport into water systems.[2] Additionally, up to 90% of phosphate fertilizers can be retained in soils, but the fraction that is mobilized by surface runoff also contributes to eutrophication and ammonium pollution. Livestock farming and the improper management of animal manure have also been identified as significant sources of ammonium in agricultural watersheds.[4,5] In addition to agricultural non-point sources, municipal wastewater treatment plants and industrial effluents can directly release ammonium-rich discharges into nearby water bodies, contributing to ammonium pollution.[6]

Ammonium pollution can disrupt the balance of nitrogen cycles in aquatic ecosystems, leading to eutrophication. This process results in excessive growth of algae, which depletes oxygen levels in water bodies, harming aquatic life.[7] The accumulation of ammonium ions can also affect the physiological processes of aquatic organisms, leading to increased mortality rates among sensitive species.[8] Moreover, the leachate from landfills, which often contains high concentrations of ammonium, poses a risk to groundwater quality, further complicating the environmental impact of ammonium pollution.[9] The leachate can migrate into surrounding water sources, introducing pollutants that threaten ecological and human health.[10]

Recent studies have explored various methods for treating ammonium in wastewater, focusing on both biological and physical adsorption techniques. One prominent biological method is using microalgae for phytoremediation, which has demonstrated high removal efficiencies for ammonium, achieving up to 99.8% in aquaculture wastewater.[11] In addition to biological methods, adsorption has emerged as a highly effective approach for ammonium removal. Several materials have been investigated for their adsorption capacities, including natural zeolites and agricultural by-products. For

[a]*Department of Chemistry, Hanoi Pedagogical University 2, 32 Nguyen Van Linh, Xuan Hoa, Phuc Yen, Vinh Phuc, Vietnam*
[b]*Center for Advanced Technology Development, Thai Nguyen University, Tan Thinh Ward, Thai Nguyen City, Vietnam. E-mail: vanhuutap@tnu.edu.vn*

© 2025 The Author(s). Published by the Royal Society of Chemistry

Open Access Article. Published on 30 April 2025. Downloaded on 6/15/2026 5:50:00 AM. This article is licensed under a Creative Commons Attribution-NonCommercial 3.0 Unported Licence.

instance, calcined natural zeolite modified with sodium nitrate has been shown to effectively remove ammonium from aqueous solutions, highlighting its potential as a low-cost adsorbent.[12] Recent research has demonstrated that chemically modified zeolites, such as those treated with ethylenediaminetetraacetic acid (EDTA), significantly enhance the removal of ammonium from aqueous solutions.[13] Moreover, Na–zeolite, when applied in flow-electrode capacitive deionization systems, has demonstrated dual functionality in ammonium removal and nutrient recovery, highlighting its potential for sustainable agricultural applications.[14] Novel materials, including cellulose sulfate nanofibers, have emerged as innovative alternatives to traditional adsorbents, exhibiting superior ammonium sorption capacities compared to conventional materials like zeolites.[15] Similarly, polyurethane sponges have been effectively utilized for ammonium removal, with adsorption kinetics strongly influenced by solution pH and ionic strength.[16] Furthermore, organic waste materials, such as banana peel powder, have shown promise as cost-effective adsorbents for ammonium ions, underscoring the potential of low-cost biomass-derived alternatives.[17]

Furthermore, recent research has indicated that coffee husk, a by-product of coffee processing, can be an efficient ammonium adsorbent, demonstrating significant removal capabilities.[18] Biochar derived from exhausted coffee husk has been identified as an effective adsorbent, demonstrating significant removal efficiency under varying carbonization conditions.[19] Moreover, its production through low-temperature pyrolysis enhances its adsorption capacity, which is primarily attributed to its highly porous structure and substantial surface area.[20] Polyaniline (PANi), a conducting polymer, has also been studied for its ammonium adsorption properties. Its unique structure enhances interaction with ammonium ions, making it a promising material for wastewater treatment applications. The combination of PANi with other materials, such as biochar, has been explored to improve adsorption efficiency further, showcasing the versatility of these materials in addressing ammonium pollution.[18]

In recent years, the composite material of coffee husk and polyaniline (PANi) has not been extensively studied for ammonium adsorption, presenting a novel area for research. This study aims to synthesize a composite material, designated as CF@PANi, combining coffee husk with PANi to enhance the adsorption capacity for ammonium ions from aqueous solutions. Coffee husk, a widely available agricultural by-product, has demonstrated potential as an effective adsorbent due to its high surface area and porous structure.[21] Incorporating PANi, a conducting polymer known for its excellent adsorption properties, is expected to improve further the composite's efficiency in removing ammonium from wastewater. The development of CF@PANi as an adsorbent could provide a sustainable solution for ammonium pollution, leveraging the abundant availability of coffee husks while enhancing their functionality through polymer modification. The innovative use of CF@PANi as an adsorbent is anticipated to improve the efficiency of ammonium removal due to the synergistic effects of the porous structure of coffee husk and the conductive properties of PANi.

This research aims to utilize the composite material CF@PANi, which integrates coffee husk and polyaniline, for the adsorption of ammonium ions from aqueous solutions. This study will systematically evaluate several factors influencing the adsorption process, including the ratio of coffee husk to PANi in the composite, the pH of the ammonium solution, the adsorption time, the mass of the adsorbent, and the initial concentration of ammonium. Moreover, the research will assess the kinetics and isotherms of ammonium adsorption by CF@PANi, aiming to elucidate the underlying mechanisms involved in the adsorption process.

Materials and methods

Material preparation

Synthesis of the PANi/coffee husk composite material involves several systematic steps to ensure effective polyaniline (PANi) integration with coffee husk sourced from Dak Lak province, Vietnam. Initially, the coffee husk is thoroughly cleaned to eliminate dust and soil contaminants, then drying in an oven at 105 °C for 24 hours. Once dried, the husk is ground into a fine powder with a uniform particle size ranging from 0.5 to 1 mm, which is crucial for maximizing the surface area available for adsorption.

The synthesis process begins with dissolving 4.6 mL of aniline in 200 mL of 1 M HCl under controlled conditions, maintaining a temperature between 0 °C and 5 °C by a magnetic stirrer (SK-300 – South Korea) to prevent premature polymerization. The prepared coffee husk is then added to the aniline solution at predetermined mass ratios of PANi to coffee husk, specifically 1 : 1, 1 : 2, and 1 : 3. The mixture is stirred continuously for 20 min, ensuring that the temperature remains within the specified range.

Subsequently, ammonium persulfate is gradually introduced into the mixture at a molar ratio of 1 : 1 with aniline, initiating the oxidative polymerization of aniline. The reaction proceeds for 18 h under low-temperature conditions, facilitated by the magnetic stirrer to ensure homogeneity and complete polymerization. After polymerization, the composite material is filtered using a vacuum pump and washed with acetone and methanol (1 : 1) to remove unreacted aniline and by-products.

Following purification, the composite is immersed in a 0.5 M ammonia solution for 2 h to neutralize residual acid. The final product is then filtered and dried in an oven at 50–60 °C for 4 h, resulting in the PANi/coffee husk composite material, CF@PANi. This innovative material is anticipated to exhibit enhanced adsorption properties for ammonium ions, making it a promising candidate for wastewater treatment applications.

The synthesis process is designed to prioritize recovery and reuse as key strategies for minimizing environmental impact. Specifically, the ammonia solution and washing solvents, including acetone and methanol, are systematically collected and reintegrated into subsequent synthesis batches, leading to a substantial reduction in waste discharge. Furthermore, any residual liquid waste containing nitrogen compounds is subjected to comprehensive treatment through well-established chemical techniques, such as microbial denitrification or

Open Access Article. Published on 30 April 2025. Downloaded on 6/15/2026 5:50:00 AM. This article is licensed under a Creative Commons Attribution-NonCommercial 3.0 Unported Licence.

precipitation, prior to disposal. These measures ensure full compliance with rigorous environmental standards, enhancing the sustainability of the overall process.

Batch adsorption experiment

The initial experimental conditions were meticulously established, utilizing an adsorbent material mass of 0.03 g, corresponding to a concentration of 0.6 g L^{-1}. The adsorption process was conducted over 20 min, with an initial ammonium concentration set at 20 mg L^{-1}. Batch adsorption experiments were performed in 100 mL glass conical flasks, each containing 50 mL of ammonium solution at ambient temperature (25 ± 2 °C). The experimental parameters examined included the influence of the ratio of polyaniline (PANi) composition to coffee husk (CF) on the adsorption efficiency of NH_4^+ at the specified initial concentration, as well as variations in the initial pH of the ammonium solution (ranging from 3 to 9), the duration of adsorption (from 5 to 120 min), the mass of the adsorbent (ranging from 0.2 to 3 g L^{-1}) and the initial ammonium concentration (spanning from 5 to 60 mg L^{-1}).

All adsorption experiments were conducted on a shaker operating at 120 rpm, utilizing the magnetic stirrer (SK-300 – South Korea) under controlled room temperature conditions. After adsorption, samples were centrifugated and filtered through filter paper to ascertain the ammonium concentration. The concentration of ammonium before and following the adsorption process was quantified using UV-vis molecular absorption spectroscopy (V730, Jasco – Japan) at a wavelength of 450 nanometers, with the calibration curve defined by the equation $y = 0.1053x - 0.0004$, demonstrating a high correlation coefficient ($R^2 = 0.9991$). Each experimental trial was conducted in triplicate to ensure the reliability of the results, with the outcomes averaged for further evaluation. Data analysis and processing were executed utilizing Microsoft Excel, while graphical representations of the adsorption data and models were generated using Origin 2024. The data points depicted in the graphs are presented as the mean ± standard deviation, thereby providing a comprehensive overview of the variability and reliability of the experimental results.

Adsorption kinetic and isotherm models

The NH_4^+ adsorption capacity onto CF@PANi at a given time t (q_t, mg g^{-1}) and at equilibrium (q_e, mg g^{-1}) was calculated using the following formulas:

$$q_t = \frac{(C_o - C_t)V}{M} \quad (1)$$

$$q_e = \frac{(C_o - C_e)V}{M} \quad (2)$$

where C_0, C_t and C_e (mg L^{-1}) represent the concentrations of NH_4^+ at the start, at any time t, and equilibrium, respectively; V (L) is the volume of the NH_4^+ solution used; and M (g) refers to the dry mass of the CF@PANi.

Two well-established models were applied to examine the adsorption kinetics of NH_4^+ onto CF@PANi – the pseudo-first-order and pseudo-second-order models. The mathematical expressions for these models are provided below:

$$\ln(q_e - q_t) = \ln q_e - k_1 t \quad (3)$$

$$\frac{t}{q_t} = \frac{1}{k_2 q_e^2} + \frac{1}{q_e} t \quad (4)$$

where q_e, q_t (mg g^{-1}) are the adsorption capacity at equilibrium and at time t (min), respectively; k_1 (min^{-1}) and k_2 (g mg^{-1} min^{-1}) are the rate constant of the pseudo-first-order and pseudo-second-order models, respectively;

In this context, q_e and q_t (mg g^{-1}) represent the adsorption capacities at equilibrium and a specific time t (min). The rate constants k_1 (min^{-1}) and k_2 (g mg^{-1} min^{-2}) correspond to the Pseudo-first-order and Pseudo-second-order models.

The Langmuir and Freundlich models were applied to describe the adsorption isotherms of NH_4^+ onto CF@PANi. The Langmuir model assumes that adsorption occurs on a monolayer surface, where the energy of the active sites is uniform and constant. On the other hand, the Freundlich model suggests that adsorption takes place on a heterogeneous surface, with active sites having diverse energy levels. The mathematical representations for the Langmuir and Freundlich models are provided by eqn (5) and (6), respectively.

$$q_e = \frac{q_m K_L C_e}{1 + K_L C_e} \quad (5)$$

$$q_e = K_F C_e^{\frac{1}{n}} \quad (6)$$

Here, q_e and q_m (mg g^{-1}) represent the equilibrium and maximum adsorption capacities, respectively; C_e (mg L^{-1}) denotes the concentration of NH_4^+ in the solution at equilibrium; K_L (L mg^{-1}) is the Langmuir constant; K_F (mg g^{-1}) is the Freundlich constant, and n is the adsorption intensity.

Results and discussion

Characteristics of CF@PANi

The Scanning Electron Microscopy (SEM) and Energy Dispersive X-ray Spectroscopy (EDS) analyses of (CF@PANi) before and after ammonium adsorption reveal significant morphological and compositional changes, providing insights into the adsorption mechanism and the material's potential applications. Before ammonium adsorption, the SEM image (Fig. 1(a1)) illustrates a compact and uniform surface morphology characterized by closely packed clusters and minimal porosity. This observation indicates that the pristine CF@PANi possesses a stable framework with well-organized structures, which may serve as potential active sites for adsorption. Following ammonium adsorption, the surface morphology undergoes notable transformations, becoming rougher and more porous, with increased irregularities (Fig. 1(b1)). These structural modifications suggest a strong interaction between ammonium ions and the active sites on the material's surface. The observed surface roughness and enhanced porosity likely result from structural rearrangements or swelling of the polymeric framework during adsorption, further confirming the effectiveness of CF@PANi as an adsorbent.

© 2025 The Author(s). Published by the Royal Society of Chemistry

Open Access Article. Published on 30 April 2025. Downloaded on 6/15/2026 5:50:00 AM. This article is licensed under a Creative Commons Attribution-NonCommercial 3.0 Unported Licence.

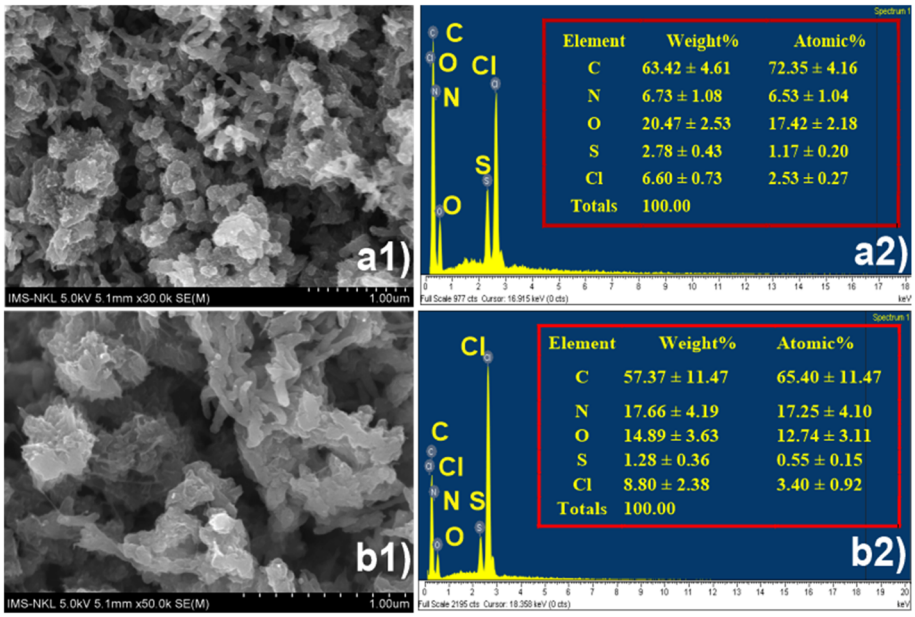

Fig. 1 SEM image and EDS spectra of CF@PANi before (a1 and a2) and after ammonium adsorption (b1 and b2).

The EDS analysis provides quantitative evidence of ammonium adsorption. Before adsorption, the elemental composition of CF@PANi includes carbon (63.42 ± 4.61%), nitrogen (6.73 ± 1.08%), oxygen (20.47 ± 2.53%), sulfur (2.78 ± 0.43%) and chlorine (6.60 ± 0.73%) (Fig. 1(a2)). The nitrogen content primarily originates from the CF@PANi, which contains nitrogen-rich functional groups capable of interacting with ammonium ions. After ammonium adsorption, a substantial increase in nitrogen content to 17.66 ± 4.19% is observed, accompanied by a decrease in carbon content to 57.37 ± 11.47% (Fig. 1(b2)). This significant rise in nitrogen indicates successful adsorption of ammonium ions, as the nitrogen peak now reflects contributions from both the CF@PANi and the adsorbed ammonium. Also, the increase in chlorine content from 6.60 ± 0.73% to 8.80 ± 2.38% may be attributed to residual chloride ions from the ammonium chloride source, further validating the interaction between the material and ammonium ions. These compositional changes highlight the pivotal role of nitrogen-rich functional groups and the CF@PANi framework in facilitating ammonium adsorption.

The combined SEM and EDS results underscore the high adsorption efficiency of CF@PANi and its structural adaptability during the adsorption process. The morphological changes, including increased surface roughness and porosity, coupled with the compositional shifts, such as the elevated nitrogen content, provide clear evidence of strong ammonium adsorption. These findings emphasize the material's potential for practical applications in environmental remediation, particularly in ammonium removal from wastewater. The dual contribution of the polyaniline matrix and the PANi-based framework enhances the material's adsorption capacity, making CF@PANi a promising candidate for efficient and sustainable water treatment solutions.[22,23]

The characterization of CF@PANi through the BET analysis, FTIR spectroscopy, and the pH_{PZC} analysis (Fig. 2) provides a comprehensive understanding of its surface area, functional groups and surface charge properties, essential for evaluating its adsorption performance. The nitrogen adsorption–desorption isotherm (Fig. 2a) exhibits a Type IV isotherm with a noticeable hysteresis loop, indicative of a mesoporous structure. The CF@PANi demonstrates a specific surface area of 7.0642 $m^2\ g^{-1}$, a pore volume of 0.040351 $cm^3\ g^{-1}$ and an average pore size of 22.5419 nm, reflecting moderate porosity that is suitable for the adsorption of larger molecules or ions. Although the surface area is not exceptionally high, the mesoporous structure facilitates better accessibility to adsorption sites, potentially enhancing interactions with adsorbates.[24]

The FTIR spectra in Fig. 2b provide comprehensive insights into the functional groups present on the surface of CF@PANi and their active role in NH_4^+ adsorption. Before adsorption, several characteristic peaks are observed. The broad peak at 3446 cm^{-1} corresponds to the O–H stretching vibration, indicative of hydroxyl groups, with its broad nature, suggesting the presence of hydrogen-bonded hydroxyl groups that serve as potential active sites for adsorption. Peaks at 2925–2855 cm^{-1} are attributed to C–H stretching vibrations from aliphatic chains, representing structural components of the coffee husk (CF) and the polyaniline (PANi) framework. The peak at 1619 cm^{-1} is associated with the stretching vibrations of aromatic C=C bonds within the polyaniline structure, highlighting the presence of conjugated aromatic rings. Moreover, 1382–1299 cm^{-1} peaks correspond to C–N stretching vibrations, confirming the presence of nitrogen-containing groups, such as amine (–NH, $–NH_2$), critical for chemical interactions during adsorption. Other peaks, such as those at 1114 cm^{-1} and 505 cm^{-1}, are attributed to C–H out-of-plane bending and skeletal vibrations of the polyaniline matrix, respectively.

© 2025 The Author(s). Published by the Royal Society of Chemistry

Open Access Article. Published on 30 April 2025. Downloaded on 6/15/2026 5:50:00 AM.
This article is licensed under a Creative Commons Attribution-NonCommercial 3.0 Unported Licence.

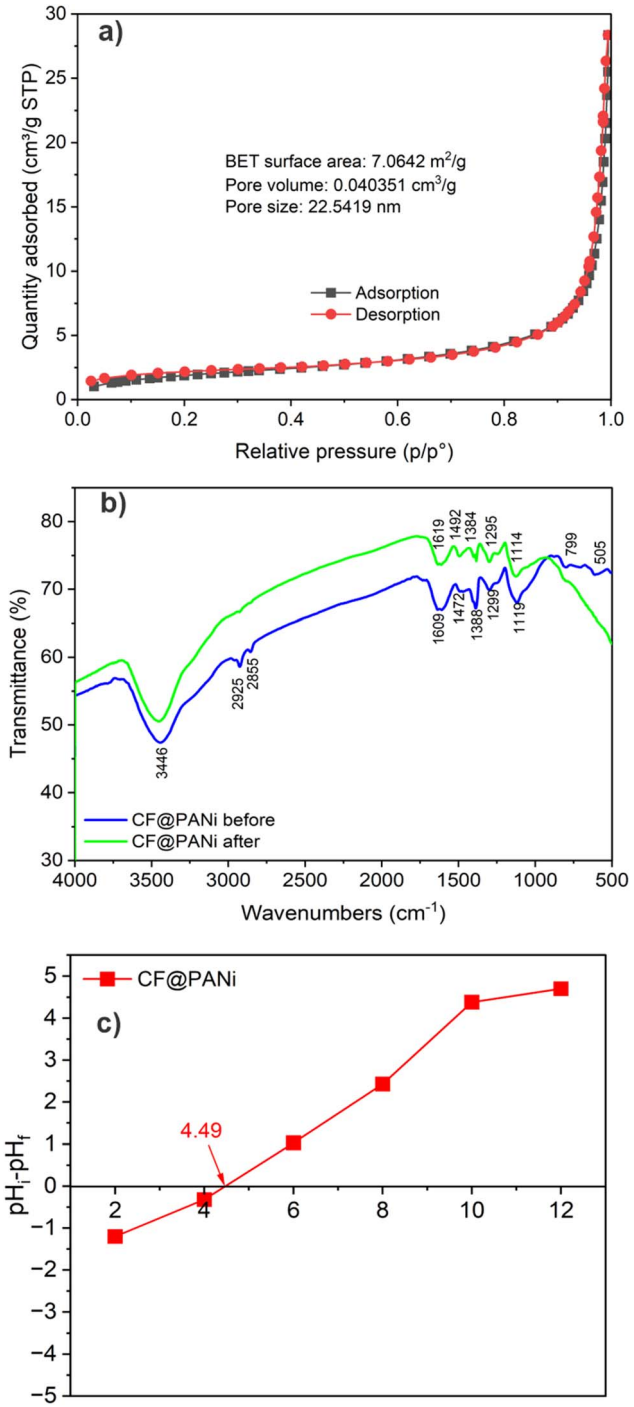

Fig. 2 BET analysis (a), FTIR (b) and pH_{PZC} (c) of CF@PANi.

After ammonium adsorption, notable changes occur in the FTIR spectra. The broad O–H peak at 3446 cm^{-1} shifts slightly and changes in intensity, confirming the involvement of hydroxyl groups in hydrogen bonding or electrostatic interactions with NH_4^+ ions. Similarly, the peaks at 1619 cm^{-1} and 1382–1299 cm^{-1} exhibit shifts and changes in intensity, indicating that aromatic rings (C=C) and nitrogen-containing functional groups (C–N, –NH, $–NH_2$) actively participate in binding NH_4^+. These groups likely form electrostatic interactions or surface complexes with ammonium ions, underscoring their critical role in adsorption. Also, the increased intensity of nitrogen-associated peaks reflects the incorporation of ammonium ions into the structure, as confirmed by the EDS analysis, which shows a significant rise in nitrogen content after adsorption.[25]

Moreover, the pH_{PZC} analysis (Fig. 2c) reveals a value of approximately 4.49, indicating that the surface of CF@PANi is positively charged at pH values below 4.49 and negatively charged at pH above 4.49. This dual charge behaviour enhances its versatility, enabling the adsorption of anions at lower pH levels and cations at higher pH levels, thus making it adaptable to various environmental conditions.[23] Overall, CF@PANi exhibits a balanced set of properties, including a mesoporous structure, active functional groups, and adaptable surface charge, collectively positioning it as a promising candidate for adsorption applications. Despite its moderate surface area, the mesoporous nature and chemical functionalities compensate for this limitation, allowing for strong adsorption performance across varying conditions. These findings suggest that CF@PANi holds significant potential for use in environmental remediation, particularly in the removal of contaminants from wastewater.

Effect of PANi and CF ratio on ammonium adsorption

The experiment aimed at determining the optimal ratio of polyaniline (PANi) to coffee husk (CF) was conducted and illustrated in Fig. 3. The effect of the PANi-to-CF ratio on ammonium (NH_4^+) adsorption efficiency is depicted in Fig. 3, highlighting the significant influence of composite composition on adsorption performance. At a PANi : CF ratio of 1 : 1, the adsorption efficiency (H) is approximately 40%, indicating moderate performance likely due to the limited amount of PANi present in the composite, thereby reducing the availability of nitrogen-containing functional groups (such as –NH and $–NH_2$)

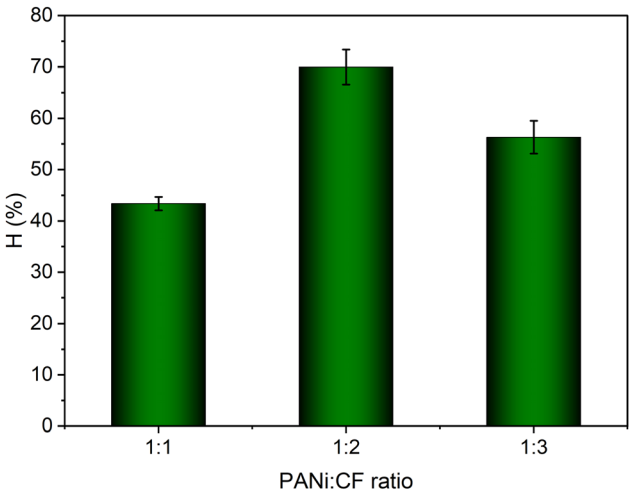

Fig. 3 The effect of the ratio of PANi composition to the CF on NH_4^+ adsorption efficiency; experimental conditions: initial NH_4^+ concentration 20 mg L^{-1}; adsorbent dosage 0.6 g L^{-1} and pH 7, contact time of 20 min.

© 2025 The Author(s). Published by the Royal Society of Chemistry

Open Access Article. Published on 30 April 2025. Downloaded on 6/15/2026 5:50:00 AM. This article is licensed under a Creative Commons Attribution-NonCommercial 3.0 Unported Licence.

responsible for substantial interaction with NH_4^+. Increasing the PANi : CF ratio to 1 : 2 results in a marked improvement in adsorption efficiency, reaching approximately 70%. This significant increase can be attributed to the enhanced presence of PANi in the composite, providing more active sites for ammonium binding. This is consistent with the expected synergy between the conductive polyaniline matrix and the porous structure of the coffee husk. However, when the ratio is further increased to 1 : 3, the adsorption efficiency decreases slightly to about 60%. This decline suggests that excessive PANi content in the composite might lead to aggregation or reduced exposure of active sites, thereby diminishing the material's overall adsorption efficiency.

These findings align with prior studies, demonstrating that optimal adsorption efficiency was often achieved with a balanced ratio of components in hybrid materials. For instance, research involving polyaniline composites with bio-based materials has reported that an excess of the conductive polymer can negatively affect surface area and porosity, limiting access to active adsorption sites.[22,26] Furthermore, the experimental conditions used in this study – an initial NH_4^+ concentration of 20 mg L^{-1}, adsorbent dosage of 0.6 g L^{-1}, pH 7, and a contact time of 20 min – ensure that the comparison was valid and provides a realistic evaluation of the material's performance under typical environmental conditions.[27] Therefore, the PANi : CF ratio of 1 : 2 was identified as the optimal composition for achieving the highest NH_4^+ adsorption efficiency under the given conditions. This highlights the importance of balancing the conductive polymer and the bio-based support material to maximize synergistic effects, ensuring an ideal combination of surface area, porosity and active site availability. Thus, the PANi : CF ratio of 1 : 2 has been identified as the optimal composition for achieving the highest ammonium ion (NH_4^+) adsorption efficiency under the specified experimental conditions. This optimal ratio was utilized to synthesize the CF@PANi material for subsequent experiments conducted in this study.

Effect of solution pH on ammonium adsorption using CF@PANi

The effect of pH on NH_4^+ adsorption efficiency (H%) and adsorption capacity (q) using the CF@PANi is illustrated in Fig. 4, underscoring the critical role of pH in determining adsorption performance. The experiment was conducted under controlled conditions with an initial NH_4^+ concentration of 20 mg L^{-1}, an adsorbent dosage of 0.6 g L^{-1}, and a contact time of 40 minutes. The results demonstrate an explicit dependency of both H% and q on the solution pH, which is closely linked to the surface charge characteristics of CF@PANi and the speciation of NH_4^+ ions.

At a pH of 3, the H% is recorded at 43.40%, with the q of 14.47 mg g^{-1}, representing the lowest performance within the studied pH range. This diminished adsorption efficiency can be attributed to the protonation of the surface functional groups of CF@PANi. The material's point of zero charge (pH_{PZC}) is approximately 4.49, indicating that at pH levels below this

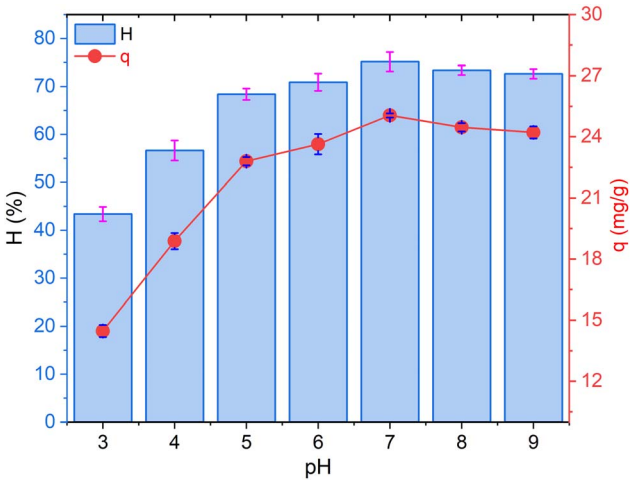

Fig. 4 The effect of pH solution on NH_4^+ adsorption efficiency using CF@PANi; experimental conditions: initial NH_4^+ concentration 20 mg L^{-1}; adsorbent dosage 0.6 g L^{-1}, contact time of 40 min.

threshold, the surface of CF@PANi becomes positively charged. This positive charge leads to electrostatic repulsion between the positively charged NH_4^+ ions and the adsorbent surface, significantly hindering adsorption.[24]

As the pH increases to 4 and 5, a notable improvement in adsorption performance is observed. At the solution pH 4, H% rises to 56.65% and q increases to 18.88 mg g^{-1}. By pH 5, the H% and q improve to 68.40% and 22.80 mg g^{-1}, respectively. This enhancement can be attributed to the reduction in surface protonation as the solution pH approaches the pH_{PZC}, which minimizes electrostatic repulsion and facilitates stronger interactions between NH_4^+ ions and the active functional groups on CF@PANi, such as amine (–NH) and hydroxyl (–OH) groups.[25]

The optimal adsorption performance is observed at pH 7, where H% reaches 75.15% and q achieves its maximum value of 25.05 mg g^{-1}. At this neutral pH, the surface charge of CF@PANi is near zero, which minimizes repulsive forces and allows the functional groups on CF@PANi to interact freely with NH_4^+ ions. At this pH, NH_4^+ predominantly exists in its ionic form (NH_4^+), facilitating strong electrostatic interactions and hydrogen bonding with the active adsorption sites on the material.[23]

However, beyond pH 7, a slight decline in adsorption performance is noted. At pH 8, H% decreases to 73.40%, and q drops to 24.47 mg g^{-1}. Similarly, at pH 9, H% and q decrease to 72.65% and 24.22 mg g^{-1}, respectively. This reduction can be explained by the deprotonation of functional groups on CF@PANi, resulting in a negatively charged surface. While the negatively charged surface may still attract positively charged NH_4^+ ions, the speciation of NH_4^+ shifts towards its neutral form (NH_3) at higher pH levels, thereby reducing the availability of NH_4^+ ions for adsorption and consequently lowering overall adsorption performance.[22]

These findings align with previous studies that have demonstrated the significant influence of pH on ammonium adsorption processes. For instance, Domingues *et al.* (2017)[26]

Open Access Article. Published on 30 April 2025. Downloaded on 6/15/2026 5:50:00 AM. This article is licensed under a Creative Commons Attribution-NonCommercial 3.0 Unported Licence.

reported that ammonium adsorption onto zeolites highly depended on pH, with optimal removal occurring at neutral pH levels. Similarly, Aragaw *et al.* (2022)[27] highlighted that the adsorption capacity of biochar for ammonium ions was significantly affected by pH, emphasizing the importance of optimizing pH conditions for effective contaminant removal.[21] Consequently, the optimal pH for ammonium adsorption has been determined to be 7, at which point the equilibrium between electrostatic interactions and the availability of functional groups is maximized. This pH condition was utilized in the subsequent experiments conducted throughout this study.

Effect of adsorption time

The influence of contact time on the adsorption efficiency (H%) and adsorption capacity (q) of NH_4^+ utilizing the CF@PANi is depicted in Fig. 5. The experiments were conducted under controlled conditions, specifically with an initial NH_4^+ concentration of 20 mg L^{-1}, an adsorbent dosage of 0.6 g L^{-1}, and a pH of 7. The results underscore the critical role of contact time in achieving adsorption equilibrium and optimizing performance.

Initially, a rapid adsorption phase is observed within the first 20 minutes. At the 5-min mark, H% reaches 48.95%, corresponding q of 16.32 mg g^{-1}. By the 10-minute interval, H% increases to 58.85%, and q rises to 19.62 mg g^{-1}, indicating a significant enhancement in adsorption capacity. This rapid uptake of NH_4^+ during the early phase can be attributed to the high availability of active sites on the CF@PANi surface, coupled with the strong driving force provided by the concentration gradient between the NH_4^+ ions in solution and the adsorbent surface. This phenomenon aligns with findings from recent studies, which have demonstrated that a high rate of solute uptake characterizes the initial stages of adsorption due to the abundance of unoccupied adsorption sites.[28,29]

As the contact time extends to 20 minutes, H% further improves to 71.95%, and q reaches 23.98 mg g^{-1}, suggesting that many adsorption sites have been utilized. After 40 min, the adsorption process reaches equilibrium, with H% achieving its maximum value of 74.9% and q stabilizing at 24.967 mg g^{-1}. Beyond this point, the changes in H% and q become minimal, as evidenced by the values recorded at 60 min (H%: 74.6%, q: 24.867 mg g^{-1}) and 120 min (H%: 73.85%, q: 24.617 mg g^{-1}). This trend indicates that adsorption is primarily governed by the saturation of available active sites and the establishment of equilibrium between the adsorbed NH_4^+ ions and the remaining ions in the solution.[30,31] The slight decrease in H% and q observed beyond the equilibrium point can be attributed to desorption effects or minor reorganization of the adsorbed ions at the material's surface. However, this reduction is negligible and does not significantly impact the overall adsorption performance. These findings suggest that a contact time of 40 min is sufficient to achieve maximum adsorption efficiency and capacity, which is essential for optimizing adsorption in practical applications.[32]

From the above results, the adsorption of NH_4^+ onto CF@PANi is strongly time-dependent, with rapid adsorption occurring within the first 20 min and equilibrium reached at approximately 40 min (H%: 74.9%, q: 24.967 mg g^{-1}). Future experiments will be conducted with a fixed adsorption time of 40 minutes to ensure optimal performance in subsequent studies.

Effect of CF@PANi weight on ammonium adsorption

The impact of CF@PANi weight on the adsorption efficiency (H%) and adsorption capacity (q, mg g^{-1}) for NH_4^+ is illustrated in Fig. 6. The experiments were conducted under controlled conditions, with an initial NH_4^+ concentration of 20 mg L^{-1}, a pH of 7 and a contact time of 40 min. The results reveal a clear relationship between the adsorbent weight and both the adsorption efficiency and capacity, which can be attributed to the interplay between the availability of adsorption sites and the equilibrium dynamics of the solution.

As the weight of the adsorbent increases from 0.01 g to 0.03 g/50 mL, the H% significantly rises from 38.3% to a peak value of 72.34%. This increase can be explained by the more

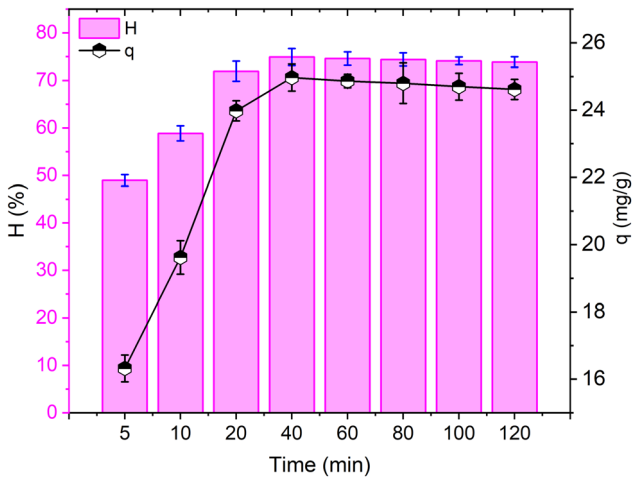

Fig. 5 Effect of contact time on the NH_4^+ adsorption efficiency using CF@PANi materials; experimental conditions: initial NH_4^+ concentration 20 mg L^{-1}; adsorbent dosage 0.6 g L^{-1}, pH 7.

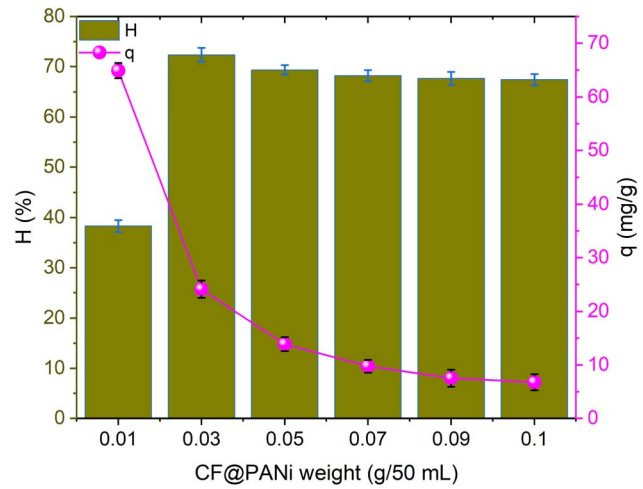

Fig. 6 Effect of CF@PANi weight on the NH_4^+ adsorption efficiency; experimental conditions: initial NH_4^+ concentration 20 mg L^{-1}; pH 7 and contact time 40 min.

© 2025 The Author(s). Published by the Royal Society of Chemistry

Open Access Article. Published on 30 April 2025. Downloaded on 6/15/2026 5:50:00 AM. This article is licensed under a Creative Commons Attribution-NonCommercial 3.0 Unported Licence.

significant number of available adsorption sites, which facilitates the removal of more NH_4^+ ions from the solution. However, when the weight exceeds 0.03 g/50 mL, *H*% plateaus, with values recorded at 69.4%, 68.25%, 67.7%, and 67.45% for weights of 0.05 g, 0.07 g, 0.09 g, and 0.1 g/50 mL, respectively. This stabilization suggests that the adsorption of NH_4^+ ions has reached equilibrium, where additional adsorbent weight does not significantly enhance removal efficiency due to the limited concentration of NH_4^+ ions remaining in the solution at equilibrium.

Conversely, the *q* exhibits a decreasing trend as the adsorbent weight increases. At 0.01 g/50 mL, *q* is at its highest, measuring 64.9 mg g^{-1}, indicating that a smaller amount of adsorbent can effectively adsorb a relatively high concentration of NH_4^+ ions. However, as the weight increases to 0.03 g, *q* sharply declines to 24.11 mg g^{-1}, decreasing to 6.745 mg g^{-1} at 0.1 g. This inverse relationship arises because the fixed amount of NH_4^+ ions in the solution becomes distributed over more adsorption sites as the adsorbent weight increases, leading to a dilution effect on the adsorption capacity per gram of adsorbent.

The combined trends of *H*% and *q* underscore the necessity of optimizing the adsorbent weight for effective adsorption. While higher weights result in increased *H*%, the diminishing returns in *q* at larger weights suggest a decrease in the adsorbent's per-gram efficiency. For instance, at 0.03 g, *H*% reaches its maximum of 72.34%, while *q* remains relatively high at 24.11 mg g^{-1}, suggesting that this weight represents an optimal balance for practical applications. Beyond this weight, although *H*% stabilizes, the sharp decline in *q* indicates an inefficient use of the adsorbent, which could be detrimental in large-scale applications.

These findings are consistent with previous studies that have explored the relationship between adsorbent dosage and adsorption performance. For example, Gao *et al.* (2018)[33] reported similar trends in the adsorption of ammonia and nitrate using chitosan–zeolite composites, where an optimal dosage was identified beyond which adsorption efficiency plateaued due to site saturation. Furthermore, while Hemmami (2024)[34] discusses the regeneration and reusability of chitosan-based adsorbents, it does not directly address the specific relationship between adsorbent weight and adsorption performance, indicating a need for further research in this area. Thus, the CF@PANi dosage of 0.03 g/50 mL, equivalent to 0.6 g L^{-1}, will continue to be used for experiments investigating the effect of the initial NH_4^+ concentration.

Effect of ammonium concentration

The adsorption behavior of CF@PANi for NH_4^+ was systematically investigated as a function of the initial NH_4^+ concentration, as illustrated in Fig. 7. The experiments were conducted under controlled conditions, specifically at a contact time of 40 min, an adsorbent dosage of 0.6 g L^{-1}, and a pH of 7. The results reveal distinct trends in adsorption efficiency (*H*%) and adsorption capacity (*q*, mg g^{-1}), highlighting the material's performance and inherent limitations.

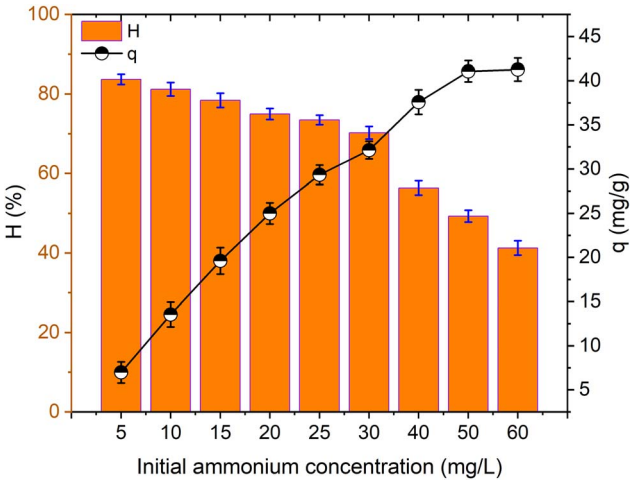

Fig. 7 Effect of NH_4^+ concentration on adsorption capacity and efficiency using CF@PANi materials, experimental conditions: contact time of 40 min; adsorbent dosage 0.6 g L^{-1}, pH 7.

The adsorption efficiency (*H*%) exhibits a decreasing trend as the initial NH_4^+ concentration increases. At a low NH_4^+ concentration of 5 mg L^{-1}, *H*% achieves its highest value of 83.72%, indicating the CF@PANi's effective capability to capture a significant proportion of NH_4^+ ions at lower concentrations. However, as the NH_4^+ concentration rises to 10, 20 and 30 mg L^{-1}, *H*% gradually declines to 81.2%, 74.95% and 70.24%, respectively. At even higher concentrations of 40, 50 and 60 mg L^{-1}, *H*% drops significantly to 56.375%, 49.28% and 41.27%. This reduction in removal efficiency can be attributed to the saturation of available adsorption sites as the NH_4^+ concentration increases, which limits the material's ability to maintain high efficiency at elevated concentrations. Similar observations have been documented in previous studies, where adsorption efficiency decreased with increasing pollutant concentration due to site saturation effects.[35,36]

In contrast, the *q* demonstrates an increasing trend with the initial NH_4^+ concentration, reflecting enhanced adsorbent utilisation at higher concentrations. At 5 mg L^{-1}, *q* is recorded at 6.98 mg g^{-1}, increasing to 24.98 mg g^{-1} at 20 mg L^{-1} and peaking at 41.27 mg g^{-1} at 60 mg L^{-1}. This trend indicates that as the NH_4^+ concentration rises, the driving force for mass transfer becomes stronger, facilitating more significant adsorption per unit mass of the adsorbent. The opposing trends of *H*% and *q* can be explained by the relationship between the adsorbent's capacity and the availability of adsorption sites. At low NH_4^+ concentrations, the active sites on the adsorbent are in excess relative to the number of ammonium ions, allowing for high removal efficiency. However, as the concentration increases, the number of NH_4^+ ions surpasses the available adsorption sites, resulting in a reduced *H*% despite the higher *q* values.

The plateau and subsequent decline in *H*% at higher concentrations suggest the approach of adsorption equilibrium, where the limited adsorption sites are nearly saturated. These findings indicate that CF@PANi performs effectively at low to moderate NH_4^+ concentrations, achieving both high

Open Access Article. Published on 30 April 2025. Downloaded on 6/15/2026 5:50:00 AM. This article is licensed under a Creative Commons Attribution-NonCommercial 3.0 Unported Licence.

efficiency and reasonable capacity. However, at very high concentrations, the efficiency drops significantly, and the adsorbent's capacity becomes the primary factor determining performance. This behavior is consistent with the findings of Duong,[37] who reported that adsorption capacity tends to increase with concentration, but the efficiency diminishes due to site saturation.

In practical terms, the results suggest that the use of CF@PANi is optimal at initial NH_4^+ concentrations below 30 mg L^{-1}, where a balance between high efficiency (H% ~70–83%) and moderate capacity (q ~25–32 mg g^{-1}) can be achieved. Additional strategies, such as increasing the adsorbent dosage or integrating complementary treatment methods, may be necessary at concentrations exceeding this threshold to maintain effective NH_4^+ removal. This aligns with the recommendations from previous studies, which advocate for optimizing operational parameters to enhance the overall performance of adsorption systems.[38,39]

Ammonium adsorption kinetics

The kinetics of ammonium ion (NH_4^+) adsorption onto the CF@PANi were systematically investigated. As illustrated in Fig. 8, the experimental data were analyzed using three kinetic models: the pseudo-first-order, pseudo-second-order and Elovich models, with the corresponding parameters summarized in Table 1. The results provide valuable insights into the adsorption mechanism and the applicability of each model in characterizing the adsorption process.

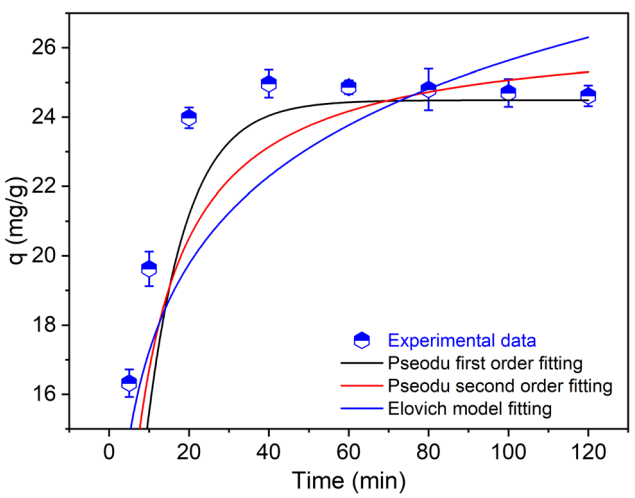

Fig. 8 Kinetic models of NH_4^+ adsorption by CF@PANi.

The experimental NH_4^+ adsorption capacity ($q_{e,\ exp}$) using CF@PANI was determined to be 9.21 mg g^{-1}, as shown in Table 1. This value is significantly different from the calculated adsorption capacity ($q_{e,\ cal}$) of 24.49 mg g^{-1} in the first order model, suggesting that the pseudo-first order model does not fully describe the adsorption kinetics in this study. On the other hand, the pseudo-second order model yields a calculated adsorption potential ($q_{e,\ cal}$) of 26.54 mg g^{-1}, which is still higher than the experimental value of 9.21 mg g^{-1}, but when combined with other parameters, it suggests a better fit for the overall kinetic behaviour. The pseudo-second order model shows significantly higher coefficient of determination (R^2 = 0.9309) than the first order model (R^2 = 0.0303), which underlines its superior suitability to represent experimental data. The predominance of the pseudo-second-order model suggests that the adsorption process is primarily governed by chemisorption, which involves valence forces or electron exchange between NH_4^+ ions and the active sites on CF@PANi. This finding is consistent with previous studies that have identified chemisorption as a key mechanism in the adsorption of ammonium ions onto various adsorbents.[28,29]

In contrast, the pseudo-first-order model poorly fits the experimental data, characterized by a rate constant (k_1) of 0.1 and a notably low R^2 value. This indicates that the adsorption process is not predominantly influenced by physisorption or diffusion-limited mechanisms, which the pseudo-first-order model typically describes. Such results align with findings from other studies that have similarly reported the inadequacy of the pseudo-first-order model in accurately representing ammonium adsorption kinetics.[30,31]

The Elovich model, with parameters a = 40.26 and b = 0.273, demonstrated the highest R^2 value of 0.9483, indicating a good fit to the experimental data. The Elovich model is often associated with heterogeneous adsorption systems, suggesting that the surface of CF@PANi contains a distribution of active sites with varying adsorption energies. The strong correlation provided by the Elovich model highlights the complexity of the adsorption process, indicating the potential involvement of both chemical and physical interactions during the adsorption of NH_4^+ ions.[32,40]

Table 1 Parameters of the kinetic models for NH_4^+ adsorption using CF@PANi

Pseudo-first-order model			Pseudo-second-order model			
$q_{e,\ cal}$ (mg g^{-1})	k_1	R^2	$q_{e,cal}$ (mg g^{-1})	k_2	R^2	$q_{e,exp}$ (mg g^{-1})
24.49	0.1	0.0303	26.54	0.0064	0.9309	9.21
Elovich model						
a			b			R^2
40.26			0.273			0.9483

© 2025 The Author(s). Published by the Royal Society of Chemistry

Open Access Article. Published on 30 April 2025. Downloaded on 6/15/2026 5:50:00 AM. This article is licensed under a Creative Commons Attribution-NonCommercial 3.0 Unported Licence.

The kinetic data further reveal that equilibrium is reached within approximately 40 min, after which a plateau is observed. The rapid initial adsorption phase can be attributed to the availability of abundant active sites on CF@PANi, which diminishes as these sites become occupied, leading to a decrease in the adsorption rate over time. This behavior is consistent with the findings of other researchers who have noted similar trends in the kinetics of ion adsorption onto composite materials.[33,34] Therefore, the pseudo-second-order model best describes the adsorption kinetics of NH_4^+ onto CF@PANi, indicating a chemisorption-dominated process. The good fit of the Elovich model further suggests surface heterogeneity and the potential for multi-mechanism interactions. These findings underscore the high efficiency and suitability of CF@PANi for ammonium adsorption under the specified experimental conditions, positioning it as a promising material for water and wastewater treatment applications.

Ammonium adsorption isotherms

The ammonium adsorption behavior of CF@PANi was evaluated using isotherm models, as illustrated in Fig. 9. The experimental data were fitted to both the Langmuir and Freundlich models, with the corresponding parameters presented in Table 2. Both models effectively describe the adsorption process, exhibiting high correlation coefficients: $R^2 = 0.9901$ for the Langmuir model and $R^2 = 0.9995$ for the Freundlich model. These results indicate that both models are suitable for characterizing the adsorption of NH_4^+ onto CF@PANi, providing valuable insights into the underlying adsorption mechanisms.

The Langmuir model is predicated on the assumption of monolayer adsorption occurring on a homogeneous surface with finite and uniform adsorption sites. According to this model, the maximum adsorption capacity (q_{max}) of CF@PANi is determined to be 72.26 mg g^{-1}, with a Langmuir constant (K_L) of 0.01 L mg^{-1}. This reflects the material's strong affinity for NH_4^+ ions. The close fit of the Langmuir model suggests that the adsorption process primarily involves specific interactions between NH_4^+ ions and the active sites on CF@PANi, forming a uniform monolayer. This finding is consistent with previous studies that have reported similar high q_{max} values for various adsorbents when targeting ammonium ions.[41]

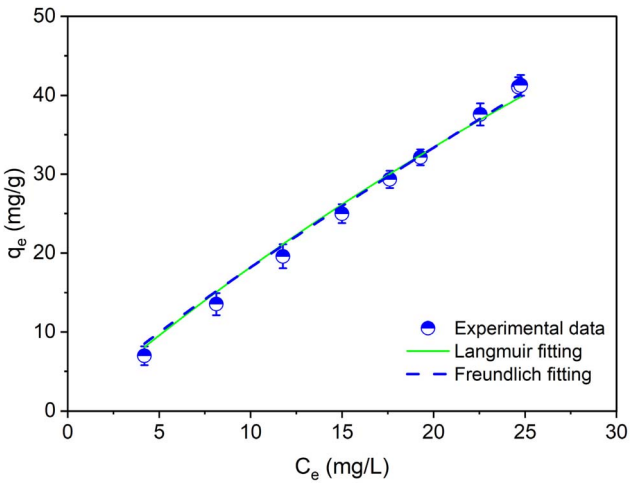

Fig. 9 Ammonium adsorption Isotherm model using CF@PANi.

Table 2 Parameters and correlation coefficients of the NH_4^+ adsorption isotherm models using CF@PANi

Langmuir model		
q_{max} (mg g^{-1})	K_L (L mg^{-1})	R^2
72.26	0.01	0.9901
Freundlich model		
K_F ((mg g^{-1})/(mg L^{-1})^n)	n_F	R^2
2.433	1.144	0.9995

In contrast, the Freundlich model accounts for adsorption on a heterogeneous surface characterized by varying affinities among the adsorption sites. The Freundlich constant (K_F) is calculated to be 2.433 ((mg g^{-1})/(mg L^{-1})^n), and the heterogeneity factor (n_F) is determined to be 1.144, indicating favorable adsorption conditions ($1 < n_F < 10$). The slightly higher R^2 value of the Freundlich model compared to the Langmuir model (0.9995 *vs.* 0.9901) suggests that surface heterogeneity and multilayer adsorption may also play a significant role in the overall adsorption process. This aligns with findings from other research indicating that heterogeneous surfaces can enhance the adsorption capacity through multilayer formation.[42]

The observed increase in adsorption capacity (q) with rising initial NH_4^+ concentration is consistent with the experimental data. At lower concentrations, abundant adsorption sites are available, leading to higher removal efficiencies. However, as the concentration increases, the available sites become occupied, and the adsorption process gradually approaches saturation. The maximum q observed in the experiments aligns well with the q_{max} predicted by the Langmuir model, further supporting the reliability of the isotherm parameters derived from the fitted models.

The above analysises indicates that the adsorption of NH_4^+ onto CF@PANi can be effectively described by both the Langmuir and Freundlich isotherm models, indicating that specific interactions and surface heterogeneity contribute to the adsorption process. These findings underscore the potential of CF@PANi as an effective adsorbent for ammonium removal in water treatment applications.

The results presented in Table 3 highlight the superior performance of CF@PANi, a novel adsorbent developed in this study, which exhibits a maximum adsorption capacity (q_{max}) of 72.26 mg g^{-1} for ammonium removal under optimal conditions of pH 7, a 40-minute contact time, and a low dosage of 0.6 g L^{-1}. This q_{max} significantly exceeds that of most previously reported materials, such as biochar from post-extraction coffee bean grounds (14.48 mg g^{-1}),[43] sorghum straw biochar (7.09 mg g^{-1})[44] and pineapple peel biochar (13.4 mg g^{-1}),[43] underscoring CF@PANi's exceptional efficiency. Even compared to synthetic

Open Access Article. Published on 30 April 2025. Downloaded on 6/15/2026 5:50:00 AM. This article is licensed under a Creative Commons Attribution-NonCommercial 3.0 Unported Licence.

Table 3 Comparison of optimal adsorption conditions and maximum adsorption capacities of the materials for ammonium removal

No	Adsorbents	q_{max} (mg g^{-1})	pH	Contact time (min)	Adsorbent dosage (g L^{-1})	References
	CF@PANi	72.26	7	40	0.6	This study
1	Biochar of post-extraction coffee bean ground	14.48	4–8	90	10	43
2	Sorghum straw biochar (SSB)	7.09	7	180	2.5	44
3	Pineapple peel biochar	13.4	7	60	8	45
4	Biochar derived from low temperature pyrolysis of coffee husk	1.64	7	360	5	49
5	Montmorillonite/Fe_3O_4	10.48	8	120	2.5	46
6	Polymer hydrogel	32.2	7	30	—	45
7	Natural clay minerals	40.84	7	30	12	48
8	Wheat straw-based amphoteric adsorbent	68.4	7	120	2	47

materials such as polymer hydrogel (32.2 mg g^{-1})[45] and montmorillonite/Fe_3O_4 (10.48 mg g^{-1}),[46] CF@PANi demonstrates a marked advantage, though it is closely rivaled by the wheat straw-based amphoteric adsorbent (68.4 mg g^{-1}).[47] Its neutral pH optimum aligns with many adsorbents, including natural montmorillonite (40.84 mg g^{-1}),[48] facilitating practical application without extensive pH adjustments. Furthermore, the 40-minute contact time of CF@PANi is notably shorter than that of materials like coffee husk biochar (360 min)[49] or Sorghum straw biochar (180 min),[44] while its minimal dosage outperforms higher requirements of alternatives such as natural clay minerals (12 g L^{-1})[48] and coffee bean ground biochar (10 g L^{-1}), enhancing its cost-effectiveness. The enhanced performance of CF@PANi likely stems from its unique structural features, such as a high surface area or abundant functional groups, which may provide more active sites for ammonium binding compared to simpler biochars or minerals. However, variations in experimental conditions across studies, such as initial ammonium concentrations or temperature, warrant caution in direct comparisons.

Mechanism of ammonium adsorption using CF@PANi

The adsorption of ammonium ions (NH_4^+) onto the CF@PANi is governed by multiple mechanisms, including electrostatic attraction, cation exchange, surface complexation, physical adsorption, and cation–π interactions (Fig. 10). These mechanisms work synergistically to optimize the capture of NH_4^+ ions. Their effectiveness is strongly influenced by the structural characteristics of CF@PANi, as revealed by various analyses, including SEM, EDS, BET surface area analysis, FTIR and pH_{PZC} assessments, alongside experimental adsorption data.

Electrostatic attraction is a critical mechanism, particularly at pH levels above the point of zero charge ($pH_{PZC} = 4.49$). At the optimal pH of 7, the CF@PANi surface is predominantly neutral or slightly negatively charged, which minimizes repulsive forces and enhances electrostatic interactions with the positively charged NH_4^+ ions. This is reflected in the high adsorption efficiency ($H = 75.15\%$) and adsorption capacity ($q = 25.05$ mg g^{-1}) observed under these conditions. The BET analysis further supports this mechanism by demonstrating a mesoporous

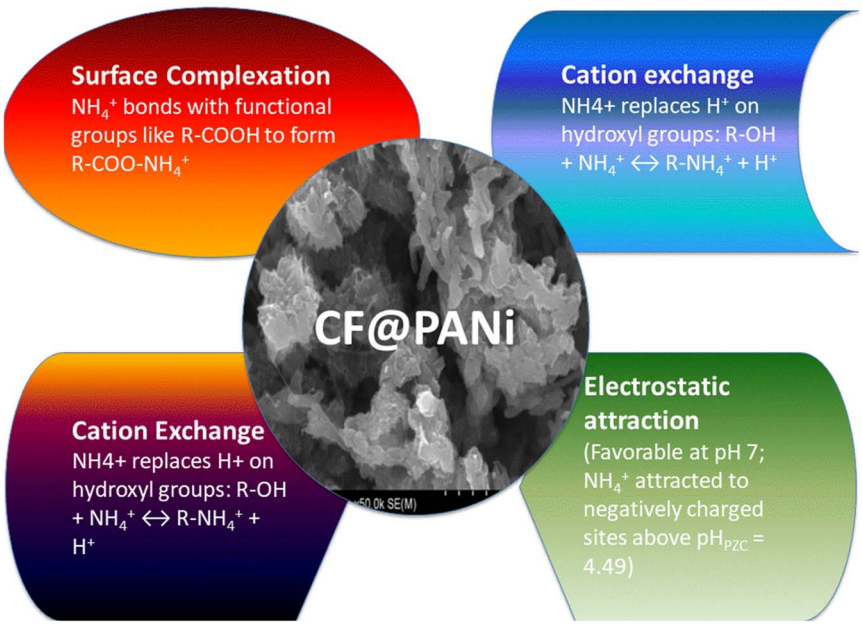

Fig. 10 Ammonium adsorption onto CF@PANi.

© 2025 The Author(s). Published by the Royal Society of Chemistry

Open Access Article. Published on 30 April 2025. Downloaded on 6/15/2026 5:50:00 AM. This article is licensed under a Creative Commons Attribution-NonCommercial 3.0 Unported Licence.

structure that facilitates effective interaction between NH_4^+ ions and the adsorbent surface.[31]

Cation exchange also plays a significant role in NH_4^+ adsorption. Functional groups such as hydroxyl (–OH) and amine (–NH, $–NH_2$) on the CF@PANi surface facilitate the exchange of NH_4^+ ions with pre-adsorbed cations, such as H^+ ions. This mechanism is particularly effective at neutral pH levels, where protonation of surface groups is minimized, enabling efficient ion exchange. The EDS results showing a substantial increase in nitrogen content (from 6.35% to 17.24%) after adsorption provide further evidence of cation exchange processes.[6]

Surface complexation enhances the adsorption capacity of CF@PANi. This mechanism involves the formation of chemical bonds between NH_4^+ ions and nitrogen-rich functional groups (such as –NH, $–NH_2$) and hydroxyl (–OH) groups on the adsorbent. FTIR spectra reveal shifts in the peaks associated with these groups after adsorption, indicating their active involvement in complexation reactions. The optimal PANi : CF ratio of 1 : 2 enhances the availability of such functional groups, as demonstrated by the significant increase in adsorption efficiency ($H = 70\%$) compared to a 1 : 1 ratio ($H = 40\%$). Physical adsorption, governed by van der Waals forces and pore filling, also contributes to the overall process. The mesoporous structure allows NH_4^+ ions to be physically trapped within the pores of CF@PANi. The SEM images before and after adsorption reveal increased surface roughness and porosity, further confirming the role of physical adsorption.[3] Finally, cation–π interactions occur between NH_4^+ ions and the delocalized π-electrons in the aromatic rings of the polyaniline matrix, as supported by studies on similar systems.[50,51] According to the study by Gallivan *et al.* (1999),[51] cation–π interactions have been confirmed to be prevalent in protein structures, where cations such as NH_4^+ can interact with aromatic rings. Meanwhile, research by Dougherty (2013)[50] demonstrated that cation–π interactions possess significant binding energy, with NH_4^+ capable of interacting with benzene at an energy of 19 kcal mol^{-1} in the gas phase. Although this energy is reduced in aqueous solutions, it remains substantial. This mechanism is particularly relevant at lower NH_4^+ concentrations, complementing electrostatic attraction and enhancing adsorption performance, as evidenced by the shifts in the FTIR peak at 1619 cm^{-1} after adsorption.

The combined contribution of these mechanisms results in the high adsorption efficiency and capacity observed for CF@PANi. The Langmuir isotherm model provides a maximum adsorption capacity ($q_{max} = 72.26$ mg g^{-1}), indicating monolayer adsorption on a homogeneous surface, while the Freundlich model suggests favorable adsorption conditions with surface heterogeneity. Kinetic studies reveal that the adsorption follows a pseudo-second-order model, indicating chemisorption as the dominant mechanism, with equilibrium reached within 40 minutes.[52]

Conclusion

The present study successfully demonstrates the development and application of CF@PANi, a composite material derived from coffee husk and polyaniline, as an efficient adsorbent for the removal of ammonium (NH_4^+) from aqueous solutions. This composite exhibits a mesoporous structure, characterized by a Brunauer–Emmett–Teller (BET) surface area of 7.0642 m^2 g^{-1} and an average pore size of 22.54 nm, and is enriched with nitrogen-containing functional groups, including amines (–NH, $–NH_2$) and hydroxyl (–OH), which are critical for the adsorption process. Experimental results indicate that CF@PANi achieves optimal adsorption performance at a pH of 7, with a PANi : CF ratio of 1 : 2 and a contact time of 40 min, resulting in a maximum adsorption capacity of 25.05 mg g^{-1}, as predicted by the Langmuir isotherm model. The kinetics of the adsorption process are described by a pseudo-second-order model, which underscores the predominance of chemisorption mechanisms, further supported by processes such as electrostatic attraction, cation exchange, surface complexation, physical adsorption and cation–π interactions. These findings highlight the potential of CF@PANi as a sustainable, cost-effective, high-performance material for ammonium removal in wastewater treatment applications. Moreover, the results provide valuable insights into the underlying adsorption mechanisms, facilitating the optimization of operational conditions for practical implementation. Future research may focus on the scalability, reusability, and regeneration of CF@PANi, thereby enhancing its applicability in real-world wastewater treatment systems. This study contributes to the advancement of eco-friendly adsorbents, addressing critical environmental challenges associated with ammonium pollution.

Future research should focus on optimizing the synthesis process through several key avenues. First, the evaluation of alternative oxidants merits attention, with studies exploring the replacement of ammonium persulfate with nitrogen-free options such as ferric chloride ($FeCl_3$), potassium iodate (KIO_3), or potassium persulfate ($K_2S_2O_8$). These substitutes could potentially eliminate ammonium generation while preserving polymerization efficiency; however, their compatibility with aniline polymerization necessitates rigorous experimental validation. Second, the development of green polymerization techniques presents a promising direction, including the use of enzymatic methods employing oxidoreductases (*e.g.*, laccase) or electrochemical approaches. These sustainable alternatives to traditional chemical oxidation could reduce or eliminate reliance on nitrogen-containing reagents, with research efforts concentrating on their scalability and cost-effectiveness for industrial application. Finally, advancements in waste treatment technologies should be pursued, such as the implementation of membrane filtration or photocatalytic degradation to address residual nitrogen compounds. These innovations could enhance the environmental sustainability of the synthesis process, moving closer to the goal of zero-discharge production.

Data availability

Data associated with this study has not been deposited into a publicly available repository. Data will be made available on request.

Open Access Article. Published on 30 April 2025. Downloaded on 6/15/2026 5:50:00 AM. This article is licensed under a Creative Commons Attribution-NonCommercial 3.0 Unported Licence.

Author contributions

Thuy-Tien Do conceived and planned the experiments; Thi-Huyen Nguyen collected, prepared nanoparticles composited coffee husk; The-Duyen Nguyen, Thuy-Tien Do, Thi-Huyen Nguyen carried out experiments; The-Duyen Nguyen, Xuan-Bach Nguyen: contributed to analysis samples before and after experimental processes; Huu-Tap Van contributed to the interpretation of the results; Huu-Tap Van, Thuy-Tien Do wrote the manuscript. All authors reviewed and revised manuscript.

Conflicts of interest

The authors have not disclosed any competing interests.

Acknowledgements

This research is funded by the Foundation for Sciences and Technology Development, Hanoi Pedagogical University 2 *via* grant number HPU2.2023-UT.15.

References

1 Y. Xia, M. Zhang, D. C. W. Tsang, N. Geng, D. Lu, L. Zhu, A. D. Igalavithana, P. D. Dissanayake, J. Rinklebe, X. Yang and Y. S. Ok, *Appl. Biol. Chem.*, 2020, **63**, 8.
2 H. Luo, X. Li, Y. Chen, X. Liu, K. Zhang, X. Fu, B. Jiang, R. Xue, J. Yang, M. Li, X. Li, W. Chen, L. Fan, F. Chen, X. Zhang and B. C. Anderson, *Int. J. Environ. Sci. Technol.*, 2022, **19**, 5493–5510.
3 X. Zhang, X. Jiang, T. Xia, X. Wei, L. Wang, L. Zhu and Z. Gao, *Pol. J. Environ. Stud.*, 2023, **32**, 4907–4918.
4 G. H. Old, P. S. Naden, S. J. Granger, G. S. Bilotta, R. E. Brazier, C. J. A. Macleod, T. Krueger, R. Bol, J. M. B. Hawkins, P. Haygarth and J. Freer, *Sci. Total Environ.*, 2012, **417–418**, 169–182.
5 A. Sibirkina, S. Likhachev, D. Dvinin, G. Voitovich, L. Trofimova, L. Markova and O. Mulyukova, *E3S Web Conf.*, 2021, **258**, 08008.
6 X. Chen, X. Shang, Z. Cheng, Z. Liu and X. Chen, *ACS Omega*, 2021, **6**, 25219–25226.
7 X. Luo, Y. Li, Q. Wu, Z. Wei, Q. Li, W. Liang, Y. Shen and R. Wang, *Int. J. Environ. Res. Public Health*, 2019, **16**, 4657.
8 Z. Chen, Z. Chang, J. Wang, Y. Liu, S. Chen and J. Li, *Aquacult. Res.*, 2021, **52**, 6656–6666.
9 A. Wdowczyk and A. Szymańska-Pulikowska, *Water*, 2020, **12**, 3129.
10 G. Przydatek, *Environ. Monit. Assess.*, 2019, **191**, 773.
11 Y. Liu, J. Lv, J. Feng, Q. Liu, F. Nan and S. Xie, *J. Chem. Technol. Biotechnol.*, 2018, **94**, 900–910.
12 H. Fu, Y. Li, Z. Yu, J. Shen, J. Li, M. Zhang, T. Ding, L. Xu and S. S. Lee, *J. Hazard. Mater.*, 2020, **393**, 122481.
13 G. A. Abelta, L. Al Qadri, M. Febrina, A. Rajak, S. Maulana, M. A. Asagabaldan and T. Taher, *Sci. Technol. Indones.*, 2024, **9**, 224–234.
14 X. He, W. Chen, F. Sun, Z. Jiang, B. Li, X. Li and L. Lin, *Environ. Sci. Technol.*, 2023, **57**, 8828–8838.
15 K. I. Johnson, W. D. Borges, P. R. Sharma, S. K. Sharma, H.-Y. Chang, M. M. Abou-Krisha, A. G. Alhamzani and B. S. Hsiao, *Nanomaterials*, 2024, **14**, 507.
16 T. Edwin, M. Mera, P. S. Komala and P. S. Zukarnaini, *IOP Conf. Ser. Earth Environ. Sci.*, 2023, **1173**, 12073.
17 R. Singh and B. Datta, *Ind. Eng. Chem. Res.*, 2022, **61**, 18464–18474.
18 J. Huang, N. R. Kankanamge, C. Chow, D. T. Welsh, T. Li and P. R. Teasdale, *J. Environ. Sci.*, 2018, **63**, 174–197.
19 A. T. Puari, A. T. Rusnam and N. R. Yanti, *IOP Conf. Ser. Earth Environ. Sci.*, 2023, **1182**, 1–10.
20 N.-T. Vu and K. Do, *Biomass Convers. Biorefin.*, 2021, **13**, 2193–2205.
21 M. Konneh, S. M. Wandera, S. I. Murunga and J. M. Raude, *Heliyon*, 2021, **7**, e08458.
22 J. Han, P. Fang, J. Dai and R. Guo, *Langmuir*, 2012, **28**, 6468–6475.
23 A. N. Doyo, R. Kumar and M. A. Barakat, *Nanomaterials*, 2023, **13**, 1014.
24 M. Adel Sayed, A. Mohamed, S. A. Ahmed, A. M. El-Sherbeeny, W. Al Zoubi and M. R. Abukhadra, *ACS Omega*, 2023, **8**, 47210–47223.
25 Z. Chen, B. Wei, S. Yang, Q. Li, L. Liu, S. Yu, T. Wen, B. Hu, J. Chen and X. Wang, *Chemistryselect*, 2019, **4**, 2352–2362.
26 R. R. Domingues, P. F. Trugilho, C. A. Silva, I. C. N. A. de Melo, L. C. A. Melo, Z. M. Magriotis and M. A. Sánchez-Monedero, *PLoS One*, 2017, **12**, e0176884.
27 T. Aragaw, S. Leta, E. Alayu and A. Mekonnen, *Adsorpt. Sci. Technol.*, 2022, 7646593.
28 M. Kapnisi, C. Mansfield, C. Marijon, A. G. Guex, F. Perbellini, I. Bardi, E. J. Humphrey, J. L. Puetzer, D. Mawad, D. C. Koutsogeorgis, D. J. Stuckey, C. M. Terracciano, S. E. Harding and M. M. Stevens, *Adv. Funct. Mater.*, 2018, **28**, 1800618.
29 K. Rekos, Z.-C. Kampouraki, C. Sarafidis, V. Samanidou and E. A. Deliyanni, *Materials*, 2019, **12**, 1987.
30 G. Galamini, G. Ferretti, V. Medoro, N. Tescaro, B. Faccini and M. Coltorti, *Ecol. Footprints Hum. Act.*, 2020, **119**, 42.
31 A. Muhammad, A. A. Shah and S. Bilal, *Materials*, 2019, **12**, 2854.
32 Y. Li, R. Xing, B. Zhang and C. Bulin, *Polym. Polym. Compos.*, 2018, **27**, 76–81.
33 Y. Gao, Y. Ru, L. Zhou, X. Wang and J. Wang, *Adv. Compos. Lett.*, 2018, **27**, 185–192.
34 H. Hemmami, I. Ben Amor, S. Zeghoud, A. Ben Amor, S. E. Laouini, A. Alsalme, D. Cornu, M. Bechelany and A. Barhoum, *Front. Chem.*, 2024, **12**, 1–14.
35 N. N. Safie, A. Z. Yaser and N. Hilal, *Asia-Pac. J. Chem. Eng.*, 2020, **15**, e2448.
36 D. Pirozzi, A. Latte, A. Yousuf, F. De Mastro, G. Brunetti, A. EL Hassanin and F. Sannino, *Nanomaterials*, 2024, **14**, 406.
37 N. B. Duong, Q. T. T. Trang, P. T. N. Bich and P. Van Lam, *Vietnam J. Chem.*, 2024, **62**, 179–186.
38 E. V Liakos, M. Mone, D. A. Lambropoulou, D. N. Bikiaris and G. Z. Kyzas, *Polymers*, 2021, **13**, 232.

© 2025 The Author(s). Published by the Royal Society of Chemistry

Open Access Article. Published on 30 April 2025. Downloaded on 6/15/2026 5:50:00 AM.
This article is licensed under a Creative Commons Attribution-NonCommercial 3.0 Unported Licence.

39 S. Zhuang and J. Wang, *Environ. Prog. Sustainable Energy*, 2018, **38**, S32–S41.
40 M. A. Khan, R. Govindasamy, A. Ahmad, M. R. Siddiqui, S. A. Alshareef, A. A. H. Hakami and M. Rafatullah, *Polymers*, 2021, **13**, 419.
41 A. M. Omer, R. Dey, A. S. Eltaweil, E. M. Abd El-Monaem and Z. M. Ziora, *Arabian J. Chem.*, 2022, **15**, 103543.
42 Z. Ma, N. Di, F. Zhang, P. Gu, S. Liu and P. Liu, *Int. J. Chem.*, 2011, **3**, 18–23.
43 H. L. Nguyen, N. Kim Chi, Le M. Tran, N. P. Dang, N. X. Tung, Do T. Tien and P. T. H. Minh, *Vietnam J. Sci. Technol.*, 2024, **62**, 324–334.
44 H. Xu, B. Wang, R. Zhao, X. Wang, C. Pan, Y. Jiang, X. Zhang and B. Ge, *Sci. Rep.*, 2022, **12**, 5358.
45 H. Cruz, P. Luckman, T. Seviour, W. Verstraete, B. Laycock and I. Pikaar, *Sci. Rep.*, 2018, **8**, 2912.
46 J. Song, V. Srivastava, T. Kohout, M. Sillanpää and T. Sainio, *Nanotechnol. Environ. Eng.*, 2021, **6**, 1–14.
47 X. Wang, S. Lü, C. Gao, C. Feng, X. Xu, X. Bai, N. Gao, J. Yang, M. Liu and L. Wu, *ACS Sustain. Chem. Eng.*, 2016, **4**, 2068–2079.
48 A. Alshameri, H. He, J. Zhu, Y. Xi, R. Zhu, L. Ma and Q. Tao, *Appl. Clay Sci.*, 2018, **159**, 83–93.
49 N.-T. Vu and K.-U. Do, *Biomass Convers. Biorefin.*, 2023, **13**, 2193–2205.
50 D. A. Dougherty, *Acc. Chem. Res.*, 2013, **46**, 885–893.
51 J. P. Gallivan and D. A. Dougherty, *Proc. Natl. Acad. Sci. U. S. A.*, 1999, **96**, 9459–9464.
52 S. F. Kuchena and Y. Wang, *ACS Appl. Energy Mater.*, 2020, **3**, 11690–11698.